Food Chemistry: X 25 (2025) 102144

Contents lists available at ScienceDirect

Food Chemistry: X

journal homepage: www.sciencedirect.com/journal/food-chemistry-x

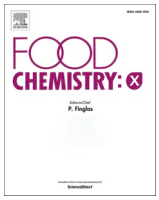

Ultrasound-assisted immersion freezing improves the digestion properties of beef myofibrillar protein

Junguang Li [a,b], Chenhao Sun [a,b], Xiaonan Yue [a,b], Wuchao Ma [a,b], Yu Wang [a,b], Jiansheng Zhao [c], Guangsu Zhu [d], Yanhong Bai [a,b,d,*]

[a] College of Food and Bioengineering, Zhengzhou University of Light Industry, Zhengzhou 450001, China
[b] Key Laboratory of Cold Chain Food Processing and Safety Control (Zhengzhou University of Light Industry), Ministry of Education, Zhengzhou 450001, China
[c] Henan Shuanghui Investment & Development Co., Ltd, Luohe 462000, China
[d] College of Food Science and Engineering, Henan University of Technology, Zhengzhou 450001, China

ARTICLE INFO

Keywords:
Beef myofibrillar protein
Ultrasound-assisted immersion freezing
Physicochemical properties
Digestion properties

ABSTRACT

This study focused on the effect of ultrasound-assisted immersion freezing (UIF) with different ultrasound power (200, 400, 600 W) on the physicochemical and *in vitro* digestive properties of beef myofibrillar proteins (BMP). The results showed that the solubility and thermal stability of BMP were significantly increased, when treated with 400 W ultrasound, and the α-helix, β-sheets, β-turns, and random-coil fractions structures content were higher and the fluorescence intensity was closest to that of the control group, demonstrating enhanced structural stability of BMP. The protein digestibility of the UIF-400 W group was significantly enhanced while the particle size of the digested product was reduced, which proved its enhanced *in vitro* digestion characteristics. Overall, UIF treatment with appropriate power can effectively delay the structural deterioration of proteins, and the loss of thermal stability, enhance the *in vitro* digestibility of proteins, and promote their digestion and utilization by consumers.

1. Introduction

Beef is an excellent source of protein, boasting an amino acid profile that aligns closely with human dietary requirements. This makes it a vital ingredient in producing premium meat products. To maintain the nutritional and processing quality of beef, freezing is the primary choice in actual processing at present. Storing meat products at low temperatures effectively slows oxidative deterioration and inhibits microbial growth, thereby extending their shelf life (Pan et al., 2021). However, freezing inevitably damages the structure of myofibrillar proteins (MP), significantly impacting gel-based muscle foods quality. In addition, the digestibility of MP, which is commonly used to assess the nutritional quality of meat products, is closely related to changes in their physicochemical properties. Traditional freezing methods include air freezing (AF) and immersion freezing (IF), in which freezing rate is normally low. Prolonged freezing often results in the formation of large and irregular extracellular ice crystals, which disrupt protein structures and degrade meat quality (Lee et al., 2024). The damage caused by ice crystals to cellular structures during freezing often leads to alterations in protein content, structural changes, and other quality impairments within the cells (Astráin-Redín et al., 2021; Pan et al., 2021). Protein denaturation readily leads to a reduction in the functional and nutritional properties of food (Zhang, Zhu, et al., 2023). During the process of slow freezing (primarily including AF and IF), the extracellular fluid, due to its low ionic concentration, freezes first to form ice crystals. This results in the creation of an osmotic pressure gradient between the intracellular and extracellular spaces (Zhang, Realini, et al., 2023). Under the influence of this osmotic pressure, water within the cells continuously migrates toward the ice crystals, ultimately leading to the formation of large and unevenly distributed ice crystals. These large ice crystals can cause irreversible damage to muscle tissue, potentially even resulting in protein denaturation (Al-Dalali et al., 2022). Therefore, it is necessary to develop new freezing technologies to enhance freezing rates, facilitate the rapid formation of small ice crystals both inside and outside cells, thereby reducing the damage to muscle structure caused by larger ice crystals and improving the quality and nutritional value of frozen meat products.

Ultrasonic-assisted immersion freezing (UIF) is an innovative rapid

* Corresponding author at: College of Food and Bioengineering, Zhengzhou University of Light Industry, Zhengzhou 450001, China.
E-mail address: baiyanhong212@163.com (Y. Bai).

https://doi.org/10.1016/j.fochx.2024.102144
Received 12 September 2024; Received in revised form 14 December 2024; Accepted 28 December 2024
Available online 30 December 2024

freezing technology that merges immersion freezing and ultrasound. This method is easy to operate, cost-effective, and non-toxic. The cavitation effect generated by ultrasound enhances ice nuclei formation, increasing the freezing rate and preserving protein structure stability (Jiang et al., 2022). Research by Zhang, Li, et al. (2023) has shown that UIF treatment can effectively slow down protein oxidation, prevent protein structure deterioration, and preserve thermal stability during frozen storage. Qiu et al. (2022) discovered that *Sciaenops ocellatus* frozen by UIF-200 W exhibited greater protein stability compared to AF and IF methods. Both ultrasonic power and frequency influence the effectiveness of UIF. Bian et al. (2022) found that multi-frequency UIF notably elevated freezing rate, reducing lipid oxidation, and preserving myofibrillar structure compared to single- and dual-frequency UIF treatments. Overall, UIF has been widely validated as a promising technique for enhancing frozen meat product quality. However, most research to date has focused on how this technology affects the structural and functional properties of MP, such as gelling and emulsifying properties. This is primarily because these properties are directly linked to the sensory qualities of meat products, including juiciness, texture, and color. However, research reports on the nutritional characteristics of frozen meat products, particularly digestibility, remain relatively scarce.

The digestive properties of MP are crucial for assessing the nutritional value of meat products. Freezing storage often results in protein degradation, which impairs MP digestibility in pork (Pan et al., 2023). However, ultrasound treatment has been shown to enhance the digestive properties of proteins. According to Jiang et al. (2022), ultrasound-treated MP from pork exhibited improved digestibility by pepsin and pancreatin and produced smaller peptides. Dong et al. (2020) found that *in vitro* shrimp protein digestibility increased with longer ultrasound treatment, from 5 to 20 min, which was due to conformational changes in proteins caused by ultrasound, which resulted in enzyme cleavage site exposure. Ultrasound has also been explored in conjunction with other modification methods to enhance the digestive properties of myofibrillar fibrillar proteins, such as glycation (Han et al., 2023) and tea polyphenols modifications (Chen et al., 2022). However, the UIF effect on the digestive properties of MP has not been thoroughly investigated. This study applied ultrasound during the meat freezing process, and comprehensively investigated the effects of UIF on the structural properties of MP as well as its impact on *in vitro* digestion characteristics.

This study aimed to investigate the effect of UIF with different ultrasound power (200, 400, 600 W) on the physicochemical and *in vitro* digestive properties of beef myofibrillar proteins. In detail, the sulfhydryl content, turbidity, solubility, and surface hydrophobicity of beef myofibrillar protein were determined. Differential scanning calorimetry (DSC) was utilized to evaluate protein thermal stability, while circular dichroism and fluorescence spectrophotometry were employed to analyze secondary and tertiary protein structures. Additionally, *in vitro* protein digestibility, as well as post-digestion particle size distribution of MP was determined. Further insights into the microstructure and molecular weight of these proteins were gained through sodium dodecyl sulfate-polyacrylamide gel electrophoresis (SDS-PAGE) and confocal laser scanning microscope (CLSM).

2. Material and methods

2.1. Materials

Fresh beef meat, specifically from the upper part of the hindquarters of *Simmental cattle*. (For each experiment, we purchased 2 kg of fresh beef from 6-month-old *Simmental cattle* at the slaughterhouse. The beef was transported to the laboratory within 24 h of slaughter, at a temperature of 4 °C.) The muscles were cut into approximately 40 mm thick slices perpendicular to the fiber direction and the weight of each sample was around 110 ± 2 (g). Pepsin and trypsin were purchased from Macklin (Shanghai, China), while all other reagents were in analytical grade.

2.2. Sample preparation

Fresh beef was portioned into polyethylene ziplock bags and placed in the refrigerator (4 °C, 6 h) to stabilize at the initial temperature. The beef sample was cut into pieces measuring 6 × 4 × 3 cm^3, with visible fat and connective tissue removed. These samples were separated into six groups for freezing treatment, comprising air freezing (AF), immersion freezing (IF), 200 W power ultrasound-assisted immersion freezing (UIF-200 W, 8.33 W/cm^2), 400 W power ultrasound-assisted immersion freezing (UIF-400 W, 16.67 W/cm^2), and 600 W power ultrasound-assisted immersion freezing (UIF-600 W, 25 W/cm^2). Specifically, the AF group was placed directly into a constant temperature freezer (Haier Special Electric Freezer Co., Ltd., China) for freezing (−20 ± 1 °C). For IF and UIF treatments, an SJT-2-10 L ultrasonic-assisted freezing equipment manufactured (Shangjia Biotechnology Co., Ltd., China) was utilized. The IF group was performed in the immersion freezing bath (−20 ± 1 °C) without ultrasound. In the UIF group, the samples were frozen with varying power levels (200, 400, and 600 W) in the freezing bath. Ultrasound frequency was set at 20 kHz, with a cycle of 5 s on and 5 s off. When the center temperature of the sample reaches 0 °C, ultrasound is turned on, and ultrasound stops when the center temperature of the sample reaches −18 °C. Subsequently, samples were rapidly transferred to a constant temperature freezer at −20 ± 1 °C. After being frozen in a constant temperature freezer for 24 h, the samples were thawed in a 4 °C freezer until the center temperature reached 4 °C for testing. The control group comprised fresh beef kept at 4 °C for 6 h.

2.3. Beef myofibrillar protein preparation

Beef myofibrillar proteins (BMP) were extracted from beef hindquarter bit according to the methods reported by Li, Ma, et al. (2022). Beef samples were trimmed of fat and connective tissue and ground in a meat grinder. Minced meat was homogenized with 10 mM phosphate buffer (2 mM $MgCl_2$, 0.1 M NaCl, 0.1 M EGTA, pH 7.0, 4 °C) at 1:4 (*w/v*) and centrifuged (3000 ×*g*, 15 min, 4 °C). After repeating this process twice, the sample was filtered through three layers of gauze. The resulting precipitation was rinsed with 0.1 M NaCl (4 °C) at 1:4 (w/v) and centrifuged under equivalent conditions, this washing step was repeated 3 times. BMP was finally obtained with concentration determined by the biuret method with bovine serum albumin as the standard protein. For subsequent analytical tests, the protein concentration was adjusted using 10 mM phosphate buffer (containing 0.6 M NaCl, pH 7.0).

2.4. Protein solubility

Protein solubility was assessed following the procedure described by Li, Wang, et al. (2022). The protein was diluted to 1 mg/mL and then subjected to centrifugation at 10,000 ×*g* for 20 min (4 °C), Biuret assay at 540 nm was used to determine the protein concentration of the supernatant. Protein solubility was calculated by dividing protein concentration in supernatant (C_s) by total protein concentration (C_t) before centrifugation, expressed as a percentage, according to eq. (1).

$$\text{Relative protein solubility}\ (\%) = \frac{C_s}{C_t} \times 100\% \quad (1)$$

2.5. Protein turbidity

MP solution turbidity was assessed following the protocol outlined by Chen et al. (2022). BMP solution was diluted to 1 mg/mL with absorbance at 660 nm measured by TU-1810 UV spectrophotometer (Beijing Puyang General Instrument Co., Ltd., China).

2.6. Total sulfhydryl and active sulfhydryl content

Total sulfhydryl content determination in BMP was slightly modified

based on the procedure described by Sun et al. (2023). 1 mL BMP solution (1 mg/mL) was combined with 8 mL buffer solution (86 mM Tris, 90 mM glycine, 8 M urea, 4 mM EDTA, pH 8.0) and centrifuged at 10,000 ×*g* for 15 min (4 °C). The resulting supernatant (4.5 mL) was mixed with 500 μL DTNB Tris-glycine buffer (10 mM DTNB, pH 8.0) and allowed to react at 25 °C for 30 min. Absorbance was detected at 412 nm. Total sulfhydryl content was determined by a molar extinction coefficient of 13,600 M^{-1} cm^{-1} and expressed in nmol/mg protein. Reactive sulfhydryl content was assessed through the same methodology omitting urea addition to the Ellman reagent.

2.7. Thermal stability

Thermal stability was evaluated utilizing a Q20 DSC (Shanghai Lirui Scientific Instrument Co., Ltd., China) following the method by Wang et al. (2020). The thawed samples (15 ± 1 mg) were placed in a standard solid aluminum pan, then sealed and transferred to a test platform, using an empty pan as a blank control. Samples underwent heating from 25 °C to 85 °C at 5 °C/min under a nitrogen atmosphere. To determine enthalpy and peak transition temperature, a linear baseline was established from the onset to the end of the exothermic curve. Peak temperature (T_{max}) and enthalpy change (ΔH) were then recorded.

2.8. Secondary structure

BMP secondary structure was conducted using a Chirascan circular dichroism spectrometer (Applied Photophysics Ltd., UK). The specimen solution was diluted to 0.1 mg/mL. Ultrapure water served as background, automatically subtracted during the measurement process. Spectra were collected across 200–260 nm with bandwidth and scan rates were set to 5 nm and 100 nm/min, respectively. Measurements were performed in triplicate, and the secondary structure content was analyzed using CDNN software provided with the instrument.

2.9. Intrinsic fluorescence spectroscopy

BMP intrinsic fluorescence was assessed utilizing an RF-6000 fluorescence spectrophotometer (Hitachi Co., Japan) with minor adjustments following the method described by Deng et al. (2023). BMP solution concentration was adjusted to 0.1 mg/mL. Sample fluorescence intensity was measured at the emission wavelength of 300–400 nm with an excitation wavelength of 280 nm employing 2000 nm/min scanning speed. Broadband for both excitation and emission was set to 3 nm.

2.10. Surface hydrophobicity

BMP surface hydrophobicity was detected using bromophenol blue method (Li et al., 2021). BMP solution (2 mg/mL) 2 mL was combined with 40 μL bromophenol blue (BPB) (1 mg/mL, pH 6.0) then centrifuged at 4000 ×*g* for 15 min (4 °C). Supernatant absorbance was detected at 595 nm by a UV spectrophotometer. The surface hydrophobicity was computed following eq. (2).

$$\text{Bound BPB}\ (\mu g) = 40 \times \frac{OD_{control} - OD_{sample}}{OD_{control}} \quad (2)$$

where $OD_{control}$ and OD_{sample} were the absorbance readings of blank group and BMP samples, respectively.

2.11. In vitro protein digestion

BMP *in vitro* protein digestion was conducted following the protocols outlined by Wen et al. (2015). BMP solution concentration was adapted to 30 mg/mL, achieved by adding 10 mM HCl solution. The mixture solution was homogenized at 9500 rpm for 30 s. Enzymatic digestion commenced in a water bath shaker at 37 °C for 120 min upon 1 mg/mL pepsin (dissolved in 10 mmol/L HCl) addition and pH adjustment to 2. Afterward, the digestion solution pH was raised to 7.5 with 1 M NaOH to deactivate pepsin. Following this, an appropriate amount of trypsin was added, and digestion proceeded in a water bath shaker at 37 °C for 2 h. Digested products were subjected to heat treatment in boiling water for 10 min to deactivate the enzyme and subsequently cooled to room temperature. Subsequently, the mixture underwent centrifugation at 11,000 ×*g* for 15 min, after which supernatant and precipitate were harvested and preserved at −18 °C for the following analysis.

2.12. In vitro protein digestibility

In vitro protein digestibility was assessed following the method by Cao et al. (2022) with certain adjustments. The digested solution was combined with ethanol at 1:3 and left at 4 °C for 12 h. Subsequently, samples were centrifuged at 10,000 ×*g* for 15 min at 4 °C and the supernatant was discarded. *In vitro,* digestibility was detected utilizing bisulfite. Protein digestibility was computed following eq. (3).

$$\text{Protein digestibility}\ (\%) = \frac{W_1 - W_2}{W_1} \times 100 \quad (3)$$

where W_1 and W_2 represent protein amount before and after digestion, respectively.

2.13. Particle size

The digested solution was diluted to 1 mg/mL, and the mean size and particle size distribution of the pepsin and trypsin mixture were detected by NANO-ZS90 laser particle sizer (Malvern Laser Particle Sizer, USA).

2.14. SDS-page

Simulated BMP pre-digestion and post-digestion proteins through gastric and gastric-intestinal digestion were characterized using SDS-PAGE according to the method by Wang et al. (2022). Precipitate was homogenized in extraction buffer 4 mL (2 % SDS, 0.01 mol/mL PBS, pH 7.0) followed by centrifugation (5000 ×*g*, 15 min, 4 °C). Resulting supernatant was combined with loading buffer at 1:4, and then heated at 95 °C for 5 min. Sample 10 μL was loaded onto 12 % separator gel and 5 % concentrator gel, running at 80 V for 10 min, then 120 V for 60 min. Coomassie Brilliant Blue R250 stained the gel for 2 h. Finally, the destained gel was photographed using a Bio-Rad gel imager (Laboratories Inc., USA). At least two replicates were performed for each sample.

2.15. Digestive samples microstructure

Samples of microstructure before and after digestion were examined using CLSM 880 laser confocal microscope (Carl Zeiss Microscope Systems, Germany). Following the fluorescent staining methodology outlined by Bai et al. (2023), stomach and intestinal samples (5 mg/mL) 2 mL were added with rhodamine dye solution 10 μL, incubated in the light-shedding room for 5 min. Stained protein solution 20 μL was immediately dripped onto a glass slide, capturing images by × 40 objective and 633 nm helium-neon laser for protein visualization.

2.16. Statistical analysis

Unless specified otherwise, each experiment was replicated three times. Results are presented as mean ± standard error. Statistical analysis was performed using analysis of variance (ANOVA) followed by Duncan's new multiple range ($p < 0.05$) using SPSS software 21.0 (IBM Inc., USA).

3. Results and discussion

3.1. Protein solubility

Protein solubility serves as a critical parameter in heat-induced gelation formation, offering insight into the protein aggregation state (Kong et al., 2023). As shown in Fig. 1a, the solubility of BMP was significantly decreased after freezing, which was attributed to the aggregation of proteins induced by freezing. The AF group had the lowest solubility of all the treatment groups at only 35.5 ± 2.12 %, since freezing leads to the destruction of muscle tissue, which promotes protein denaturation and accelerates protein aggregation (Atani et al., 2022). Besides, the partial unfolding of the conformation of the protein due to hydrophobic interactions leads to reduced protein-water interactions and ultimately reduced protein solubility (Pan et al., 2022). Protein solubility (55.50 ± 0.70 %) in the UIF-400 W cohort exhibited a significant increase compared to IF, UIF-200 W, and UIF-600 W groups ($p < 0.05$). This suggests that optimal ultrasound power mitigates protein spatial structure disruption and minimizes macromolecular protein aggregation, leading to enhanced proteolysis. Freezing with ultrasound has been shown to accelerate the freezing rate, effectively inhibiting protein aggregation. However, high ultrasound power can lead to protein denaturation and decreased solubility, which may be related to the more reactive thiol exposure and oxidation measured later in this article. According to Qiu et al. (2022), a decline in myofibrillar protein solubility during freezing primarily arises from hydrogen bonds and disulfide bond formation.

3.2. Protein turbidity

Turbidity can represent the degree of change in the scattering or absorption of light through a substance to become opaque light. As shown in Fig. 1b, the turbidity of BMP after five freezing treatments was significantly increased compared to the control group. The decrease in myofibrillar protein solubility post-freezing was attributed to oxidative denaturation, leading to heightened intermolecular hydrophobic interactions. Notably, turbidity values observed in UIF-200 W and UIF-400 W groups were notably lower ($p < 0.05$) compared to both AF and IF groups devoid of ultrasound application. This suggests that judicious UIF effectively suppresses BMP aggregation. However, the treatment effect of UIF-200 W was not as good as that of UIF-400 W. This was because the ultrasonic power (UIF-200 W) was too low, resulting in poor cavitation effects that were insufficient to effectively inhibit the formation of large ice crystals during the freezing process (Li et al., 2024). Conversely, the UIF-600 W group exhibited the highest turbidity value, possibly stemming from accelerated protein denaturation induced by high-intensity ultrasound. This culminated in protein aggregation and heightened turbidity, consistent with solubility findings. The cavitation phenomena such as shear and turbulence generated by the appropriate ultrasonic power disrupt protein-protein interactions, thereby reducing protein particle size and protein turbidity.

3.3. Total sulfhydryl and active sulfhydryl groups

Sulfhydryl groups present on protein side chains are highly reactive and readily undergo dehydrogenation to form disulfide bonds, thereby facilitating protein molecules' cross-linking. These groups are involved in maintaining spatial protein structure stability, with alterations in sulfhydryl groups serving as protein denaturation degree indicators. Fig. 2 illustrates BMP total sulfhydryl content following freezing treatment. Remarkably, a significant reduction in total sulfhydryl content was observed post-freezing treatment ($p < 0.05$). Compared to the control group (73.62 ± 0.51 μmol/g), a substantial reduction in total sulfhydryl content was evident in all freezing treatment groups, with AF groups exhibiting the lowest levels at 55.54 ± 0.24 μmol/g BMP. Notably, the UIF-400 group displayed the highest total sulfhydryl content (66.19 ± 0.32 μmol/g BMP). This trend can be attributed to small and uniform ice crystal formation during rapid freezing, which induces less damage to BMP spatial structure. Furthermore, disulfide bond formation facilitates intramolecular/intermolecular cross-linking,

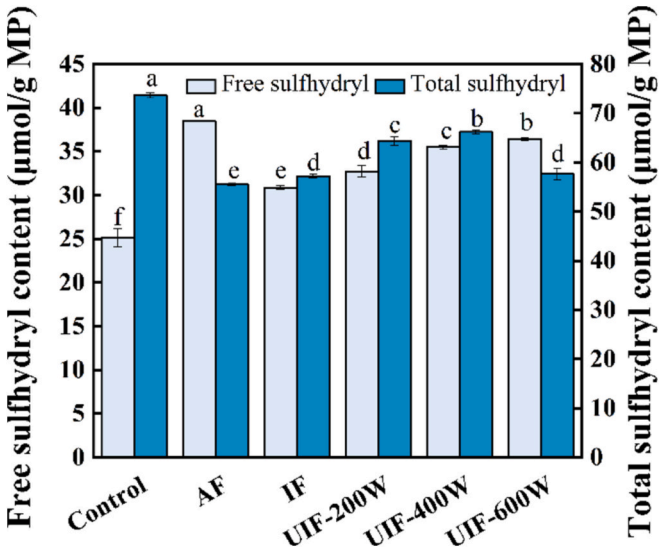

Fig. 2. Different freezing treatments impact on the content of sulfhydryl groups. Different superscripts indicate significant differences ($p < 0.05$).

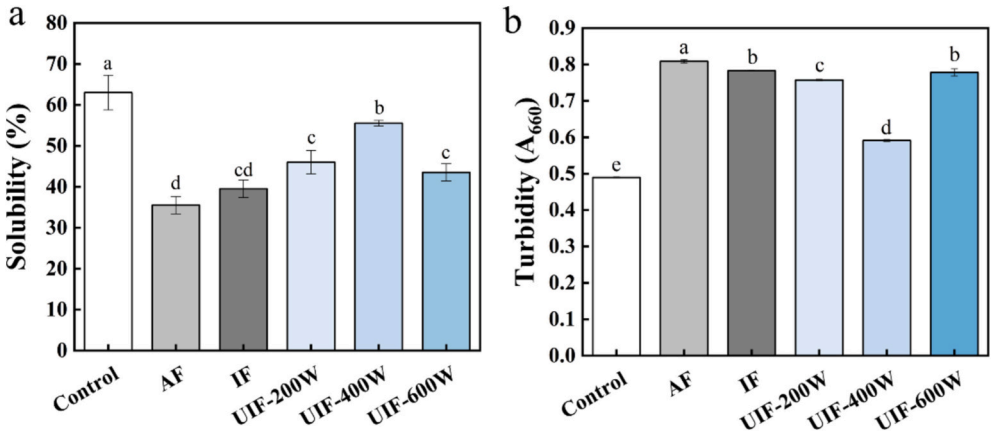

Fig. 1. Different freezing treatments impact on BMP solubility (a) and turbidity (b). Different superscripts indicate significant differences ($p < 0.05$).

promoting aggregation and compromising protein structural integrity, ultimately leading to a decrease in total sulfhydryl content (Tong et al., 2023). Additionally, as depicted in Fig. 2, a significant increase in active sulfhydryl content post-freezing treatment was observed, attributed to internal sulfhydryl exposure groups induced by protein structure unfolding (Yu et al., 2023). The process of slow freezing results in the deformation of the muscle tissue, thereby exposing more buried sulfhydryl groups. Consequently, the AF group exhibited the highest active sulfhydryl content (38.45 ± 0.05 μmol/g BMP) among the cryo-treated groups. Active sulfhydryl content exhibited an upward trend with increasing ultrasound power from 200 W to 400 W, followed by a decline as ultrasound power further increased to 600 W. This observation suggests that ultrasound treatment induced BMP structural unfolding, consequently exposing sulfhydryl groups and augmenting free sulfhydryl content. Conversely, the diminished free sulfhydryl content observed in the UIF-600 W group may be attributed to disulfide bond formation.

3.4. Thermal stability

BMP thermal stability under various treatments was assessed using DSC, with expressed T_{max} and ΔH as indicators. As shown in Table.1, the T_{max1} and T_{max2} values of all samples with freezing treatment were significantly decreased compared to the control group. This phenomenon implies that freezing heightens protein susceptibility to thermal denaturation, likely attributed to side chain groups of hydrophobic amino acids exposure during freezing. The proximity of T_{max1} and T_{max2} values in AF samples to those in the UIF-600 W group suggests that protein structures in both AF and UIF-600 W samples are less stable compared to other treatment groups. This instability may result from subunit dissociation and protein denaturation. This demonstrates that excessively high ultrasonic power not only failed to inhibit protein degradation but also disrupted protein structure, leading to protein denaturation. Moreover, the significantly higher T_{max1} and T_{max2} observed in the UIF-400 W group compared to other freezing treatment groups could be attributed to the beneficial effect of appropriate ultrasound power, which inhibits protein primary structure oxidation and prevents the formation of carbonyl groups and di-tyrosine. This mechanism enhances protein thermal stability during freezing. The decrease in both ΔH_1 and ΔH_2 values across all samples post-freezing ($p < 0.05$) may be attributed to the formation and enlargement of ice crystals, disrupting protein structure and weakening hydrogen bonds. AF group exhibited lower ΔH_1 and ΔH_2 values compared to other treatment groups, indicative of compromised protein conformation due to the formation of large and irregular ice crystals during slow freezing. On the contrary, the UIF-400 W group exhibited the highest ΔH_1 and ΔH_2 values than those of the other freezing treatment groups. The findings suggest that suitable ultrasonic power fosters the formation of smaller ice crystals and preserves the structural integrity of proteins, thereby attenuating the decline in thermal stability typically observed during protein freezing.

Table 1
Impact of various freezing treatments on BMP thermal stability.

	Myosin		Actin	
Treatment	T_{max1} (°C)	ΔH_1 (J/g)	T_{max2} (°C)	ΔH_2 (J/g)
Control	63.99 ± 0.14^{a}	0.73 ± 0.04^{a}	78.79 ± 0.23^{a}	0.46 ± 0.03^{a}
AF	58.72 ± 0.13^{d}	0.30 ± 0.06^{cd}	78.23 ± 0.10^{b}	0.16 ± 0.03^{c}
IF	60.10 ± 0.47^{bc}	0.28 ± 0.05^{cd}	78.05 ± 0.23^{b}	0.36 ± 0.06^{b}
UIF-200 W	59.74 ± 0.25^{c}	0.35 ± 0.01^{c}	78.54 ± 0.03^{a}	0.45 ± 0.02^{a}
UIF-400 W	60.80 ± 0.43^{b}	0.52 ± 0.01^{b}	78.56 ± 0.04^{a}	0.44 ± 0.04^{a}
UIF-600 W	58.24 ± 0.53^{d}	0.24 ± 0.04^{d}	78.15 ± 0.13^{b}	0.35 ± 0.02^{b}

Different superscripts indicate significant differences ($p < 0.05$).

3.5. Secondary structure

Circular dichroism spectroscopy stands as a vital tool for discerning alterations in protein secondary structures. As depicted in Fig. 3a, circular dichroism spectra unveiled the emergence of two negative peaks at 208 nm and 222 nm, hallmarking α-helix as prevalent BMP conformation. However, different treatment methods resulted in varying degrees of upward shifts of the two negative peaks (UIF-600 W > AF > IF > UIF-200 W > UIF-400 W > Control), indicating different amounts of α-helix structure loss and varying degrees of protein denaturation. The quantification results of the secondary structure content of each sample group are presented in Fig. 3b. It was observed that freezing resulted in a variable decrease in the α-helix content of the samples, which could be attributed to the transformation of the ordered structure of the proteins into a disordered one due to ice recrystallization, water redistribution, and mechanical damage to the proteins (Liu et al., 2021). Furthermore, the observed elevations in β-sheets, β-turns, and random-coil fractions indicated an augmented inclination toward protein-protein interactions, potentially impacting protein aggregation. There was no significant difference in the α-helical structure content of BMP between the AF group (17.57 ± 0.36 %) and the UIF-600 W group (16.95 ± 0.60 %), but they were significantly lower than other treatment groups. The α-helical content in the UIF-400 W group (26.58 ± 0.67 %) surpassed that of other treatments, while the proportion of random coil content (36.44 ± 0.17 %) was the lowest. Ultrasound-induced mechanical vibrations possibly disrupting protein-protein interactions and unfolding the protein structure, but the optimal ultrasound power during freezing could mitigate freeze-induced muscle structure damage, thus restraining protein denaturation.

3.6. Intrinsic fluorescence spectroscopy

Protein intrinsic fluorescence is intimately linked to its tertiary structure, primarily arising from the excitation and emission of amino acid residues, notably tryptophan (Gao et al., 2022). As illustrated in Fig. 4a, the control group displayed the lowest fluorescence intensity, with the maximum fluorescence emission wavelength (λ_{max}) at 324 nm. However, freezing treatments induced alterations in fluorescence intensity and λ_{max}, indicating changes in the tertiary structure of myofibrillar protein. The AF group exhibited the highest fluorescence intensity and λ_{max} value of 328 nm, suggesting a red-shift in tryptophan emission. Zhang, Li, et al. (2023) found that λ_{max} red-shift signifies damage to the protein's tertiary structure due to ice crystal growth, causing some tryptophan residues to transition from the protein interior to the surface. The fluorescence intensity exhibited a tendency to increase followed by a decrease with increasing ultrasound power, with UIF-400 W showing notably lower fluorescence intensity compared to other freezing treatment groups. This decrease in fluorescence intensity can be attributed to freezing process acceleration by UIF treatment at 400 W, which subsequently inhibited protein structure unfolding, thereby reducing damage to BMP tertiary structure. Consequently, UIF treatment at 400 W effectively delayed structural changes in proteins induced by freezing, ultimately mitigating frozen beef quality deterioration (Wu et al., 2022).

3.7. Surface hydrophobicity

Surface hydrophobicity serves as a pivotal parameter that is sensitive to conformational variations in proteins, allowing for meticulous monitoring of their chemical and physical states (Zhang et al., 2021). As in Fig. 4b, AF group surface hydrophobicity markedly escalated to 14.44 ± 0.71 μg compared to the control group (10.38 ± 0.24 μg). Consistent with the results of intrinsic fluorescence, the surface hydrophobicity of the UIF-400 W group was close to that of the control group, while the surface hydrophobicity of the UIF-600 W group was reduced without significant difference from that of the UIF-200 W group. This occurrence

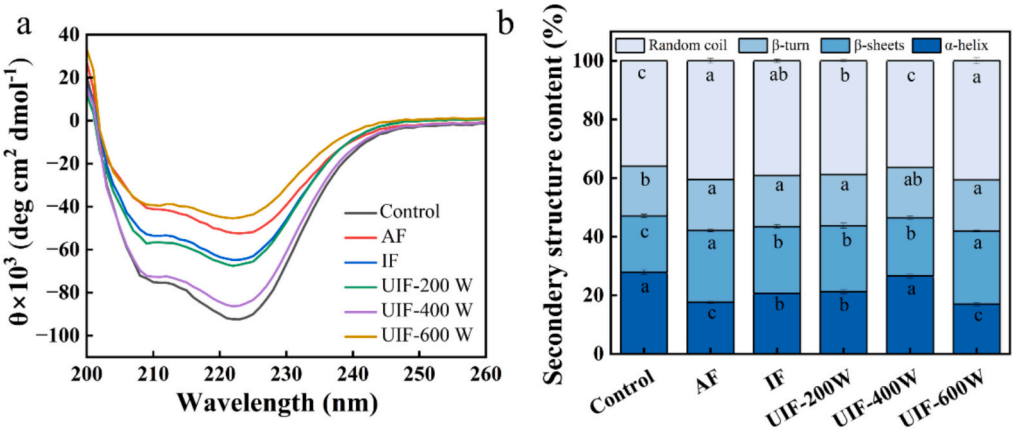

Fig. 3. Different freezing treatments impact on BMP secondary structure. Different superscripts indicate significant differences ($p < 0.05$).

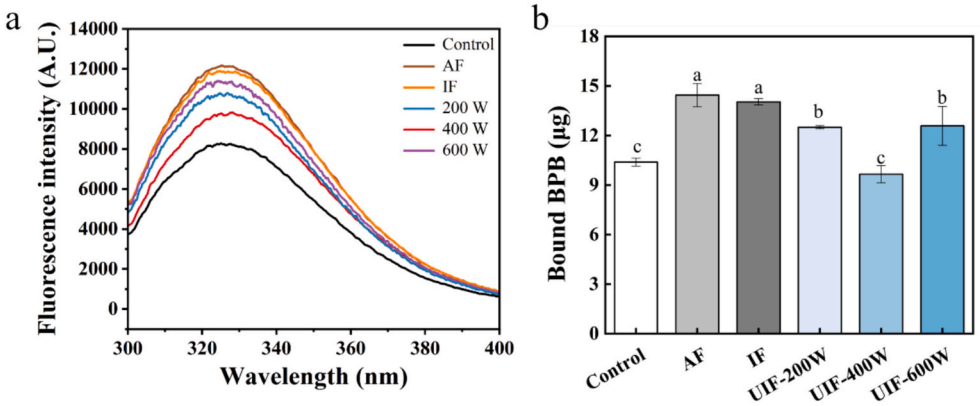

Fig. 4. Different freezing treatments impact on BMP fluorescence intensity (a) and surface hydrophobicity (b). Different superscripts indicate significant differences ($p < 0.05$).

might be ascribed to the extension and unwinding of protein molecules subsequent to the freezing treatment, leading to conformational integrity and heightened instability loss. Additionally, it was noted that gradual freezing diminishes the forces upholding protein spatial configuration, including hydrogen bonds, Van der Waals' force, and disulfide bonds, among others. Consequently, both the secondary and tertiary structures undergo alterations, unveiling internal hydrophobic residues and consequently altering hydrophobic region distribution on the protein surface (Pan et al., 2022).

3.8. *In vitro protein digestibility*

As shown in Fig. 5a, BMP was initially digested during the pepsin digestion stage. Compared to the pepsin digestion stage, the digestibility of each sample in the post-trypsin digestion stage increased significantly ($p < 0.05$), indicating that BMP was further hydrolyzed and digested under the action of trypsin. The main site of action of pepsin is the peptide bond composed of acidic or aromatic amino acids in proteins, while trypsin selectively hydrolyses the peptide chain in proteins

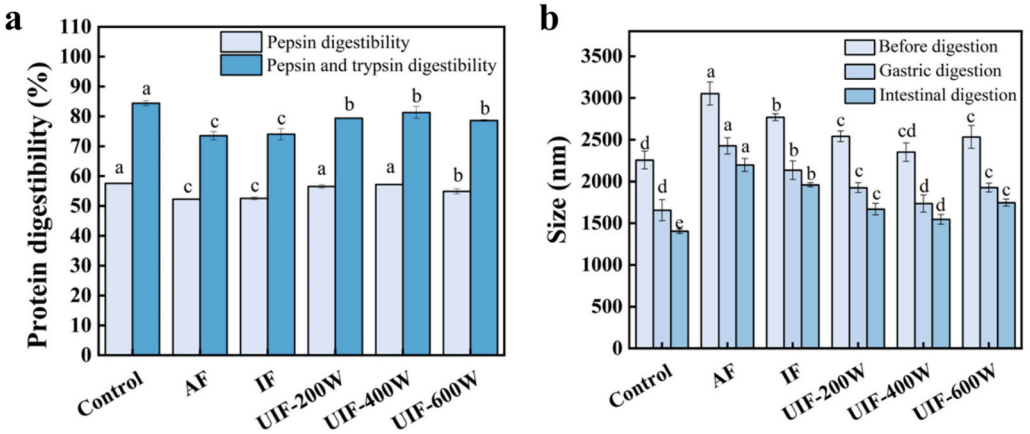

Fig. 5. Different freezing treatments impact on protein digestibility (a) and particle size before and after digestion (b). Different superscripts indicate significant differences ($p < 0.05$).

composed of lysine or arginine carboxyl groups. Denatured proteins were further hydrolyzed by trypsin based on initial digestion by pepsin, resulting in significantly increased protein digestibility (Sousa et al., 2020). In addition, the *in vitro* digestibility of BMP increased with increasing ultrasound power in both the pepsin and trypsin digestion phases, whereas the pepsin digestibility of UIF-200 W and UIF-400 W groups was closest to that of the control group. The protein digestion rate of the ultrasound treatment group was significantly higher than that of the AF and IF groups, indicating that UIF treatment was beneficial for improving the digestion characteristics of proteins. The rate of protease hydrolysis of protein was closely related to its spatial conformation. The results indicated that ultrasound can induce slight changes in BMP structure, prevent protein aggregation and denaturation, which can preserve more enzyme sites. This enhanced protease binding to BMP and improves BMP digestibility *in vitro*. In contrast, muscle structures treated by AF and IF were damaged and water was lost, leading to sclerosis of the muscle tissue, which in turn reduced protein digestibility *in vitro*. Besides, the protein solubility and turbidity results demonstrated that aggregation of proteins occurred, which reduced the sites for enzymatic digestion of proteins, ultimately leading to reduced protein digestibility. These results were similar to those obtained by Grune et al. (2004) who suggested that the creation of protein clusters alters protease recognition sites, reducing sensitivity to protein hydrolysis and affecting protein digestibility.

3.9. Particle size

As shown in Fig. 5b, the particle sizes of BMP digestion products in the freezing-treated group were all larger than in the control group. The particle size decreased and then increased with increasing ultrasonic power. When the samples were treated with UIF-400 W, the smallest particle size was observed compared to other treatment groups. Additionally, as indicated in Section 3.8, samples treated with this method exhibited higher digestibility. This indicated that protein particles with smaller particle sizes were more easily reacted by proteolytic enzymes, making them more easily absorbed by the human digestive system (Yang et al., 2023). After trypsin digestion, the particle size of BMP-digested products was further reduced, and the results of trypsin digestion were consistent with the trend of pepsin digestion. The ultrasound-treatment groups were significantly reduced compared with AF and IF groups, and the particle size tended to decrease and then increase with the increase of ultrasonic power. After hydrolysis by pepsin and trypsin, the large molecular weight protein was hydrolyzed to small molecular weight peptide or amino acid, which resulted in the reduction of the particle size of the digestive products, which was consistent with the results of SDS-PAGE (as shown in Fig. 6). The application of ultrasound could further promote BMP hydrolysis, thus reducing the particle size of the digested products.

3.10. SDS-page

The molecular weight distribution of BMP before and after digestion was evaluated by SDS-PAGE, and the major proteins in BMP include myosin heavy chain (MHC) and actin (Fig. 6). Although previous experimental results suggested that freezing can induce conformational changes in proteins, the SDS-PAGE images before digestion shown in Fig. 6 revealed no significant difference between the frozen treatment group and the control group, indicating that freezing did not cause degradation of the molecular bands and, consequently, did not alter their molecular weight (Li et al., 2020). Myosin heavy chain and actin were hydrolyzed into different peptide fragments after digestion by pepsin. In addition, pepsin showed a stronger hydrolysis of the myosin heavy chain than actin. BMP was further digested by trypsin, and the large molecular weight proteins or peptides were all completely hydrolyzed to small molecular weight peptides or amino acids. It was observed that the electrophoretic band grayscale of each frozen treatment group after the two-step digestion by stomach and trypsin was essentially devoid of clear protein bands with molecular weights less than 17 kDa compared to pre-digestion and pepsin digestion. This suggested that the protein was significantly degraded, and the results were consistent with those of ham myofibrillar protein after simulated *in vitro* gastrointestinal digestion, as reported by Paolella et al. (2015).

3.11. Digestive samples microstructure

The microstructures of undigested and digested protein products of each group were scanned using confocal laser scanning microscopy. The proteins were stained with rhodamine B and showed red fluorescent dots. As shown in Fig. 7, the amount of all samples decreased after digestion with pepsin and trypsin. This indicated that myofibrillar proteins were digested by pepsin and then further digested by trypsin to break down into small peptides. The results showed that control proteins were more easily digested and absorbed. In addition, it was observed that the protein particles of the AF and IF groups were more strongly aggregated, dispersed, and disorganized, and the particle size was considerably larger than in the control group, while the protein particles of the UIF treatment groups were more uniformly distributed, and there was no significant difference between the groups, but it was slightly

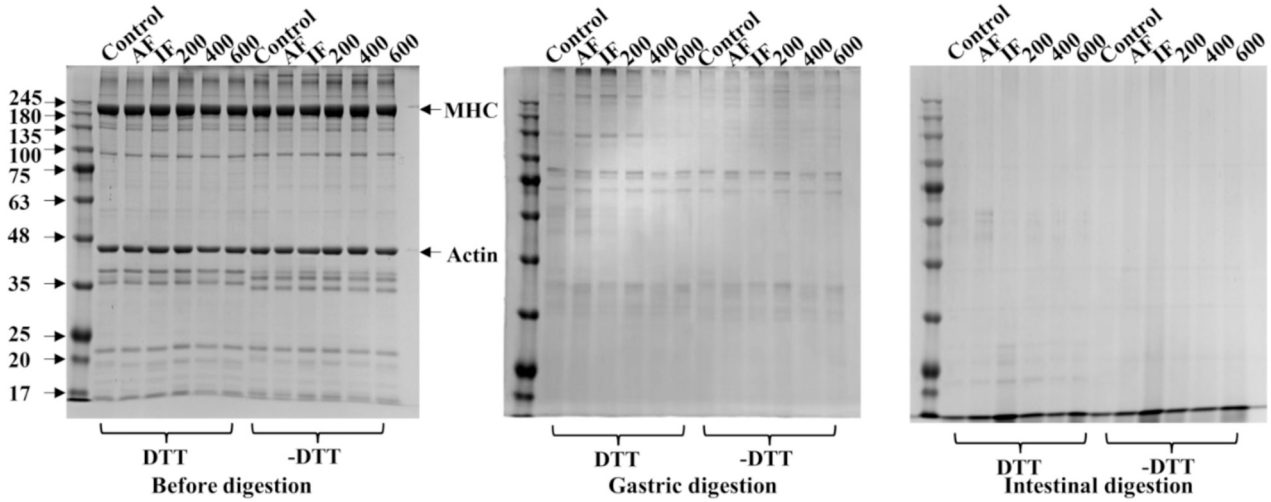

Fig. 6. Simulate the molecular weight distribution of BMP between different treatment groups before and after digestion. The numbers 200, 400 and 600 represent ultrasound-assisted immersion freezing at 200 W, 400 W, and 600 W, respectively.

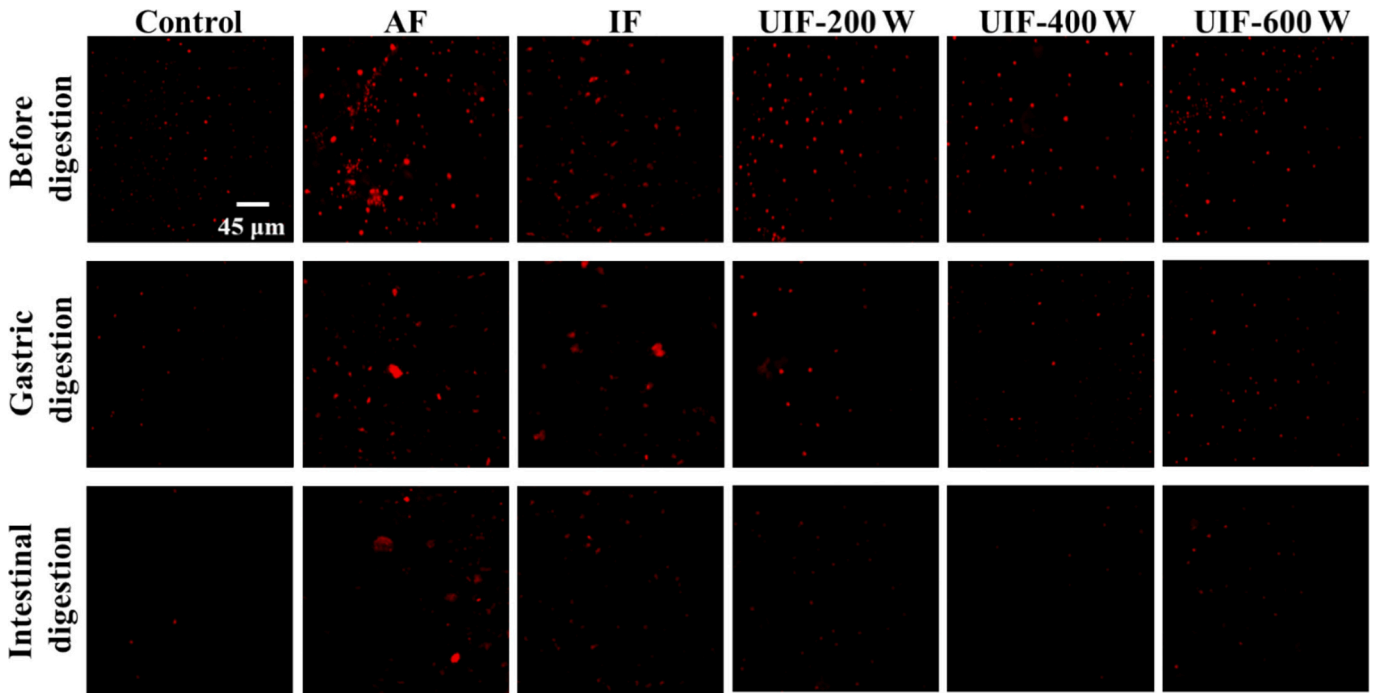

Fig. 7. Microstructure of BMP before and after digestion between in different treatment groups.

larger than that of the control group. The protein particles were reduced after gastrin digestion, but large protein particle aggregates were formed in the AF and IF groups. The large particle aggregates were obviously digested gradually after trypsin digestion, and the red spots were unclear or even not observed in the ultrasonic freezing treated group, but the red spots were more obvious in the AF group. The results showed that the protein was difficult to digest and the digestibility was reduced after freezing. Structural denaturation of proteins has been shown to lead to protein aggregation and the formation of large particles, thereby reducing protein digestibility (Choi & Chin, 2021). In addition, pepsin cleaves bonds between hydrophobic and aromatic amino acids, whereas proteins at arginine and lysine sites are cleaved by trypsin, which allows the digestion of the proteins (Li et al., 2020). However, aggregation due to protein denaturation can alter protease recognition sites, potentially reducing protease sensitivity and affecting digestibility.

4. Conclusions

In conclusion, the application of UIF was demonstrated to enhance the *in vitro* digestibility of beef myofibrillar protein (BMP). Specifically, the solubility and thermal stability of UIF-treated BMP increased and turbidity decreased, especially in the UIF-400 W group close to the control group. Furthermore, the BMP from the UIF-400 W-treated group exhibited a higher content of α-helical structure (26.58 %) and a stronger intrinsic fluorescence intensity, which proved that the UIF-treated protein was more stable. In addition, UIF also showed higher digestibility of BMP in simulated *in vitro* digestion experiments, which was attributed to the unfolding of BMP molecular structure as more enzymatic sites were preserved. Therefore, the UIF is a method that can inhibit protein denaturation and provides new insights for enhancing the nutrition and digestive properties of frozen meat, and providing ideas for future research on the effects of UIF on other types of proteins or different meat sources.

CRediT authorship contribution statement

Junguang Li: Writing – review & editing, Resources, Methodology, Conceptualization. **Chenhao Sun:** Writing – review & editing, Supervision. **Xiaonan Yue:** Writing – original draft, Validation, Investigation. **Wuchao Ma:** Formal analysis. **Yu Wang:** Formal analysis. **Jiansheng Zhao:** Formal analysis. **Guangsu Zhu:** Formal analysis. **Yanhong Bai:** Project administration, Funding acquisition.

Declaration of competing interest

The authors declare that they have no known competing financial interests or personal relationships that could have appeared to influence the work reported in this paper.

Acknowledgments

This research was supported by the Central Plains Technology Innovation Leading Talent Project (244200510011) and the Science and Technology Innovation Talent Program for Universities in Henan Province (23HASTIT047).

Data availability

The data that has been used is confidential.

References

Al-Dalali, S., Li, C., & Xu, B. (2022). Effect of frozen storage on the lipid oxidation, protein oxidation, and flavor profile of marinated raw beef meat. *Food Chemistry, 376*, Article 131881. https://doi.org/10.1016/j.foodchem.2021.131881

Astráin-Redín, L., Abad, J., Rieder, A., Kirkhus, B., Raso, J., Cebrián, G., et al. (2021). Direct contact ultrasound assisted freezing of chicken breast samples. *Ultrasonics Sonochemistry, 70*, Article 105319. https://doi.org/10.1016/j.ultsonch.2020.105319

Atani, S., Hamdami, N., Dalvi-Isfahan, M., Soltanizadeh, N., & Fallah-Joshaqani, S. (2022). Effects of microwave-assisted freezing on the quality attributes of lamb meat. *International Journal of Refrigeration, 143*, 192–198. https://doi.org/10.1016/j.ijrefrig.2022.03.019

Bai, X., Shi, S., Kong, B., Chen, Q., Liu, Q., Li, Z., et al. (2023). Analysis of the influencing mechanism of the freeze–thawing cycles on in vitro chicken meat digestion based on protein structural changes. *Food Chemistry, 399*, Article 134020. https://doi.org/10.1016/j.foodchem.2022.134020

Bian, C., Yu, H., Yang, K., Mei, J., & Xie, J. (2022). Effects of single-, dual-, and multi-frequency ultrasound-assisted freezing on the muscle quality and myofibrillar protein structure in large yellow croaker (Larimichthys crocea). *Food Chemistry, X* (15), Article 100362. https://doi.org/10.1016/j.fochx.2022.100362

Cao, C., Yuan, D., Kong, B., Chen, Q., He, J., & Liu, Q. (2022). Effect of different κ-carrageenan incorporation forms on the gel properties and in vitro digestibility of frankfurters. *Food Hydrocolloids, 129*, Article 107637. https://doi.org/10.1016/j.foodhyd.2022.107637

Chen, J., Zhao, Z., Zhou, G., & Xu, X. (2022). Comparative study on the in vitro digestibility of chicken protein after different modifications. *Food Chemistry, 385*, Article 132652. https://doi.org/10.1016/j.foodchem.2022.132652

Choi, J., & Chin, K. (2021). Structural changes of meat protein of chicken sausages with various levels of salt and phosphate and their effects on in vitro digestion. *International Journal of Food Science & Technology, 56*(10), 5250–5258. https://doi.org/10.1111/ijfs.15181

Deng, X., Ni, X., Han, J., Yao, W., Fang, Y., Zhu, Q., et al. (2023). High-intensity ultrasound modified the functional properties of Neosalanx taihuensis myofibrillar protein and improved its emulsion stability. *Ultrasonics Sonochemistry, 97*, Article 106458. https://doi.org/10.1016/j.ultsonch.2023.106458

Dong, X., Wang, J., & Raghavan, V. (2020). Effects of high-intensity ultrasound processing on the physiochemical and allergenic properties of shrimp. *Innovative Food Science & Emerging Technologies, 65*, Article 102441. https://doi.org/10.1016/j.ifset.2020.102441

Gao, K., Zha, F., Yang, Z., Rao, J., & Chen, B. (2022). Structure characteristics and functionality of water-soluble fraction from high-intensity ultrasound treated pea protein isolate. *Food Hydrocolloids, 125*, Article 107409. https://doi.org/10.1016/j.foodhyd.2021.107409

Grune, T., Jung, T., Merker, K., & Davies, K. J. A. (2004). Decreased proteolysis caused by protein aggregates, inclusion bodies, plaques, lipofuscin, ceroid, and 'aggresomes' during oxidative stress, aging, and disease. *The International Journal of Biochemistry & Cell Biology, 36*(12), 2519–2530. https://doi.org/10.1016/j.biocel.2004.04.020

Han, G., Zhao, S., Liu, Q., Xia, X., Chen, Q., Liu, H., et al. (2023). High-intensity ultrasound combined with glycation enhances the thermal stability and in vitro digestion behaviors of myofibrillar protein aqueous solution. *International Journal of Biological Macromolecules, 251*, Article 126301. https://doi.org/10.1016/j.ijbiomac.2023.126301

Jiang, S., Zhang, M., Liu, H., Li, Q., Xue, D., Nian, Y., et al. (2022). Ultrasound treatment can increase digestibility of myofibrillar protein of pork with modified atmosphere packaging. *Food Chemistry, 377*, Article 131811. https://doi.org/10.1016/j.foodchem.2021.131811

Kong, D., Quan, C., Xi, Q., Han, R., Li, P., Du, Q., et al. (2023). Effects of ultrasound-assisted slightly acidic electrolyzed water thawing on myofibrillar protein conformation and gel properties of chicken breasts. *Food Chemistry, 404*, Article 134738. https://doi.org/10.1016/j.foodchem.2022.134738

Lee, S., Jo, K., Jeong, H., Choi, Y., Kyoung, H., & Jung, S. (2024). Freezing-induced denaturation of myofibrillar proteins in frozen meat. *Critical Reviews in Food Science and Nutrition, 64*(5), 1385–1402. https://doi.org/10.1080/10408398.2022.2116557

Li, D., Tan, Z., Liu, Z., Wu, C., Liu, H., Guo, C., et al. (2021). Effect of hydroxyl radical induced oxidation on the physicochemical and gelling properties of shrimp myofibrillar protein and its mechanism. *Food Chemistry, 351*, Article 129344. https://doi.org/10.1016/j.foodchem.2021.129344

Li, J., Ma, X., Wang, Y., Du, M., Wang, Y., Du, J., et al. (2022). Effects of immersion freezing on the conformational changes of myofibrillar proteins in pork under ultrasonic power densities of 0, 15, 30 and 45 WL−1. *International Journal of Food Science & Technology, 57*(5), 2896–2905. https://doi.org/10.1111/ijfs.15596

Li, J., Sun, C., Ma, W., Wen, K., Wang, Y., Yue, X., et al. (2024). The effects of assisted freezing with different ultrasound power rates on the quality and flavor of braised beef. *Foods, 13*(10), 1566. https://doi.org/10.3390/foods13101566

Li, Q., Zhao, D., Liu, H., Zhang, M., Jiang, S., Xu, X., et al. (2020). "Rigid" structure is a key determinant for the low digestibility of myoglobin. *Food Chemistry, X*(7), Article 100094. https://doi.org/10.1016/j.fochx.2020.100094

Li, X., Wang, W., Wang, S., Shen, Y., Pan, J., Dong, X., et al. (2022). The solubility and structures of porcine Myofibrillar proteins under low-salt processing conditions as affected by the presence of L-lysine. *Foods, 11*(6), 855. https://doi.org/10.3390/foods11060855

Liu, H., Zhang, J., Wang, H., Chen, Q., & Kong, B. (2021). High-intensity ultrasound improves the physical stability of myofibrillar protein emulsion at low ionic strength by destroying and suppressing myosin molecular assembly. *Ultrasonics Sonochemistry, 74*, Article 105554. https://doi.org/10.1016/j.ultsonch.2021.105554

Pan, N., Bai, X., Kong, B., Liu, Q., Chen, Q., Sun, F., et al. (2023). The dynamic change in the degradation and in vitro digestive properties of porcine myofibrillar protein during freezing storage. *International Journal of Biological Macromolecules, 234*, Article 123682. https://doi.org/10.1016/j.ijbiomac.2023.123682

Pan, N., Dong, C., Du, X., Kong, B., Sun, J., & Xia, X. (2021). Effect of freeze-thaw cycles on the quality of quick-frozen pork patty with different fat content by consumer assessment and instrument-based detection. *Meat Science, 172*, Article 108313. https://doi.org/10.1016/j.meatsci.2020.108313

Pan, N., Wan, W., Du, X., Kong, B., Liu, Q., Lv, H., et al. (2022). Mechanisms of change in emulsifying capacity induced by protein denaturation and aggregation in quick-frozen pork patties with different fat levels and freeze–thaw cycles. *Foods, 11*(1), 44. https://doi.org/10.3390/foods11010044

Paolella, S., Falavigna, C., Faccini, A., Virgili, R., Sforza, S., Dall'Asta, C., et al. (2015). Effect of dry-cured ham maturation time on simulated gastrointestinal digestion: Characterization of the released peptide fraction. *Food Research International, 67*, 136–144. https://doi.org/10.1016/j.foodres.2014.10.026

Qiu, S., Cui, F., Wang, J., Zhu, W., Xu, Y., Yi, S., et al. (2022). Effects of ultrasound-assisted immersion freezing on the muscle quality and myofibrillar protein oxidation and denaturation in Sciaenops ocellatus. *Food Chemistry, 377*, Article 131949. https://doi.org/10.1016/j.foodchem.2021.131949

Sousa, R., Portmann, R., Dubois, S., Recio, I., & Egger, L. (2020). Protein digestion of different protein sources using the INFOGEST static digestion model. *Food Research International, 130*, Article 108996. https://doi.org/10.1016/j.foodres.2020.108996

Sun, Q., Kong, B., Zheng, O., Liu, S., & Dong, X. (2023). Effect of protein structure changes during different power ultrasound thawing on emulsification properties of common carp (Cyprinus carpio) myofibrillar protein. *Ultrasonics Sonochemistry, 101*, Article 106719. https://doi.org/10.1016/j.ultsonch.2023.106719

Tong, J., Jia, R., Xia, G., Zhang, X., Zhang, S., Wei, H., et al. (2023). Influence mechanisms of different setting time at low temperature on the gel quality and protein structure of Solenocera crassicornis surimi. *Food Bioscience, 51*, Article 102344. https://doi.org/10.1016/j.fbio.2022.102344

Wang, B., Kong, B., Li, F., Liu, Q., Zhang, H., & Xia, X. (2020). Changes in the thermal stability and structure of protein from porcine longissimus dorsi induced by different thawing methods. *Food Chemistry, 316*, Article 126375. https://doi.org/10.1016/j.foodchem.2020.126375

Wang, X., Zhou, Z., & Chen, C. (2022). In vitro digestion of a mixed gel of pork muscle and resistant starch: Salt-soluble protein perspective. *Food Chemistry, 394*, Article 133478. https://doi.org/10.1016/j.foodchem.2022.133478

Wen, S., Zhou, G., Song, S., Xu, X., Voglmeir, J., Liu, L., et al. (2015). Discrimination of in vitro and in vivo digestion products of meat proteins from pork, beef, chicken. *Fisheries, 15*(21), 3688–3698. https://doi.org/10.1002/pmic.201500179

Wu, B., Qiu, C., Guo, Y., Zhang, C., Guo, X., Bouhile, Y., et al. (2022). Ultrasonic-assisted flowing water thawing of frozen beef with different frequency modes: Effects on thawing efficiency, quality characteristics and microstructure. *Food Research International, 157*, Article 111484. https://doi.org/10.1016/j.foodres.2022.111484

Yang, Y., Zheng, Y., Ma, W., Zhang, Y., Sun, C., & Fang, Y. (2023). Meat and plant-based meat analogs: Nutritional profile and in vitro digestion comparison. *Food Hydrocolloids, 143*, Article 108886. https://doi.org/10.1016/j.foodhyd.2023.108886

Yu, X., Wang, X., Zou, L., Cai, K., Pan, J., & Chen, C. (2023). Insights into the in vitro digestibility of pork myofibrillar protein with different ionic polysaccharides from the perspective of gel characteristics. *Food Chemistry, 426*, Article 136520. https://doi.org/10.1016/j.foodchem.2023.136520

Zhang, C., Li, Y., Xia, X., Sun, Q., Sun, F., & Kong, B. (2023). Changes in protein oxidation, structure, and thermal stability of chicken breast subjected to ultrasound-assisted immersion freezing during frozen storage. *Food Chemistry, 398*, Article 133874. https://doi.org/10.1016/j.foodchem.2022.133874

Zhang, G., Zhu, C., Walayat, N., Nawaz, A., Ding, Y., & Liu, J. (2023). Recent development in evaluation methods, influencing factors and control measures for freeze denaturation of food protein. *Critical Reviews in Food Science and Nutrition, 63*(22), 5874–5889. https://doi.org/10.1080/10408398.2022.2025534

Zhang, R., Realini, C., Kim, Y., & Farouk, M. (2023). Challenges and processing strategies to produce high quality frozen meat. *Meat Science, 205*, Article 109311.

Zhang, Y., Puolanne, E., & Ertbjerg, P. (2021). Mimicking myofibrillar protein denaturation in frozen-thawed meat: Effect of pH at high ionic strength. *Food Chemistry, 338*, Article 128017. https://doi.org/10.1016/j.foodchem.2020.128017